Heliyon 9 (2023) e21330

Contents lists available at ScienceDirect

Heliyon

journal homepage: www.cell.com/heliyon

Research article

Physical and CFD model used in the analysis of particles dispersion

V.M. Fernández-Pacheco [a,*], A. Fernández-Tena [b], T. Ackermann [c], E. Blanco-Marigorta [a], E. Álvarez-Álvarez [a]

[a] Energy Department, University of Oviedo, Wifredo Ricart s/n, Gijón, 33204, Spain
[b] Instituto Nacional de Silicosis, Servicio de Salud del Principado de Asturias, Minería 1, Oviedo, 33011, Spain
[c] Fachhochschule Bielefeld, University of Applied Sciences, Artilleriestr 9, Minden, 32427, Germany

ARTICLE INFO

Keywords:
CFD
Particles
Air pollution
Wind tunnel

ABSTRACT

Air pollution, representing one of the major environmental crises affecting us all, is responsible for half a million deaths each year in Europe. This research shows a numerical model based on Computational Fluid Dynamics (CFD) and a methodology for its validation allowing to know the evolution of particles in open urban environments. In this case, the model represents an area of Gijón (Asturias), specifically chosen as it serves to highlight a location at which the daily limit values of PM_{10} set by the regulations are most frequently exceeded. A numerical model has been developed at a scale of 1:10,000 to simulate the dispersion of pollutants, including particulate emissions. A physical model at the same scale was built using 3D printing. This model was tested in a wind tunnel and analysed in the four main wind directions. To carry out the tests, a particle generation system was designed and manufactured, and the necessary infrastructure was built to take measurements using an optical particle meter. Results show that the numerical model meets the expected objectives and is capable of predicting the behaviour of particle dispersion in the air. The numerical model produces results in the same order of magnitude as the physical model, although there is a tendency to underestimate the maximum values with respect to the measured ones.

1. Introduction

One of the main consequences of urban and industrial development is air pollution. This is apparently on the rise due to population growth in cities, high consumption of fossil fuels and the widespread use of automobiles. Moreover, it has been estimated that there are about 500,000 premature deaths per year in Europe due to air pollution [1]. With a view to reversing such an adverse statistic, authorities are developing strict regulations and controls to reduce emissions of air pollutants. According to the European Union, these measures should ensure a clean atmosphere, free of anthropogenic pollutants by 2030 [2].

Air monitoring is mainly based on measurements at fixed locations, in those areas or agglomerations where levels exceed legislative thresholds. However, these proposals do not take into account the values between stations or analyze the behaviour of different pollutants (PM10, CO2, NOX...) in various scenarios (geometries and meteorological conditions). It is therefore necessary to carry out pollutant dispersion studies.

* Corresponding author.
E-mail address: fernandezpvictor@uniovi.es (V.M. Fernández-Pacheco).

https://doi.org/10.1016/j.heliyon.2023.e21330
Received 25 March 2023; Received in revised form 29 September 2023; Accepted 19 October 2023

Available online 26 October 2023

Dispersion models are one of the most universally acknowledged ways to discover the behaviour of pollutants in the atmosphere [3]. Based on dispersion models, there are numerous tools used in the study of the atmospheric dispersion of pollution, highlighting codes recommended by the Environmental Protection Agency (EPA) such as AERMOD [4] and CALPUFF [5], the Spanish tool CALIOPE [6,7] and Computational Fluid Dynamics (CFD). The CFD technique offers an interesting and innovative opportunity to study the dispersion of pollutants on a small scale as it allows for modifications to be made to each component (atmospheric conditions, pollutants, geometries, etc.). The combination with laboratory wind tunnel tests will provide a complete picture of pollutant dispersion, helping to better understand the problem.

A CFD model utilizing ANSYS Fluent software was used to examine the scattering of PM_{10} in geometries measuring 1.2x0.5x0.5 m^3, equivalent to a domain of 34 million cells, with the aim of imitating a wind tunnel model [8]. The experimentation incorporated a particle emitter and a meter within the range of 1 to 10 microns, with an obstacle placed between them. The findings demonstrate that obstacles cause a rise in PM_{10} concentration regardless of speed, as a result of recirculation around the obstacles. As velocity increases, the concentration declines (the wake broadens with speed).

The ANSYS Fluent is also used to represent a 180x18x18 m^3 street model at 1:150 scale in another study [9] where RANS k-epsilon models are compared with LES, using wind tunnel measurements for validation. The results show an enhanced performance of k-epsilon except in the centre of the street canyon since LES allows to better results. LES models improve accuracy of concentration values by knowing the unsteady fluctuations and resolving the transient mixing inside the street canyon, but the problem is the associated computational cost. Along the same lines, there are other works [10] comparing the results of RANS and LES.

On a laboratory scale [11], analyzed the influence of street canyons with square buildings on pollutant flux in a wind tunnel, concluding that dispersion and flux depended on the arranged geometry, with street ventilation being determinant.

Other research [12] also used experimental models of small building dimensions to validate their CFD simulations. For this purpose, he carried out two tests with two different layouts, street canyon and large block layouts, reinforcing the importance of a building block layout in the distribution of pollutants. In addition to the layout of the buildings, vegetation appears as another determining element in the final concentration of pollutants on an urban scale. This facilitates measurements of pollutant concentration and helps see how the concentration increased with increasing vegetation density. This is in sharp contrast with a further group of studies linked to street canyons which seemed to indicate that vegetation was a positive element in reducing the concentration of pollutants [13–17] Combining a CFD model with experimental validation is the work [18] which studied the different vegetation and height patterns in the dispersion of pollutants when using street canyons. This work, together with this one [19] reveals the influence of vegetation on the diffusion of pollutants.

Another study [20] also combined numerical and experimental models to jointly analyze the impact of wind and temperature effects on pollutant dispersion in urban areas. They used 2D and 3D street canyons and experiments that obtained very similar results to the numerical model. A special feature of the study was the way in which the heating of the street walls produced a vortex that indicated higher flow lift and an improvement in the ventilation of the street.

There are also model experimental works that simulate larger neighbourhoods. An example [21] using a set of square, dense and regularly placed obstructions, simulated different neighbourhoods. Upon them, pollutant concentration measurements were carried out for different orientations, noting the importance of studies that characterize districts and urban geometries. In another work [22], a digital terrain model (DTM) was used to introduce a scale model of the city of Liberec (Czech Republic). On it, an emission point was located, and a series of concentration sensors were used to perform the analysis. Along those lines, other work [23] had already replicated the commercial district of Hamamatsucho (Tokyo, Japan) using a model of the area that was introduced in a wind tunnel. He placed 83 measurement points on it to obtain velocity and contaminant concentrations, while testing it in different meteorological conditions. The study was complemented with a field experiment in the same area of the city to validate the correlation between the data obtained in the wind tunnel and genuine conditions both of which obtained satisfactory results. There have even been studies ([24]) where different scales were tested from neighbourhood size to those found indoors in order to determine the distribution of a pollutant in wind tunnels. Along the lines of the previous one, the work also included field measurements of temperatures, wind flow and pollutant concentration.

Finally, over and above the urban scale, the emergence of a recent work [25] has been significant. Although it follows the same vein of combining CFD numerical models with wind tunnel tests to validate pollutant dispersion, it features the difficulty of the study in a mountainous region. The experiment was conducted considering the four cardinal points (north, south, east and west) as possible wind directions.

Studies based on physical models make it possible to obtain the necessary experimental data to validate complex numerical models, such as those carried out with CFD tools. In addition to large-scale models, there are numerous case studies based on small-scale models (hundreds of meters) Attempts have been made to replicate these through simulations. Moreover, nowadays, advances in 3D printing make it possible to increase the size and resolution of these models, allowing large areas of land to be represented in detail.

For this study, the Gijón region of Spain was chosen due to its high number of daily limit values in excess of PM_{10} [26]. A CFD model was developed and a physical model was created through 3D printing, both at a scale of 1:10,000. The physical model was tested in a wind tunnel, using the main wind directions. The primary aim of this study is to formulate and authenticate a three-dimensional computational fluid dynamics model to examine industrial air pollutant propagation on a larger scale.

2. CFD model

The development of a CFD model to study the behaviour of particles involves the following steps [27]: selecting the study area, geometrical model, numerical model, input data and simulation conditions.

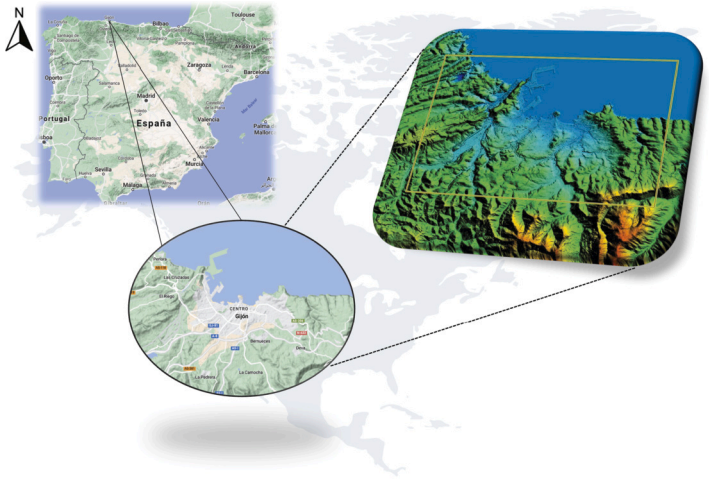

Fig. 1. Study area located in Gijón (Asturias). Source: IGN and Google Earth Pro.

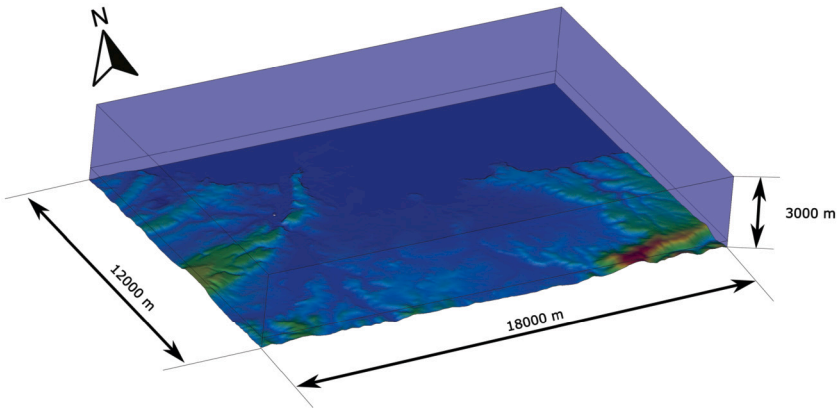

Fig. 2. Geometric model overview.

2.1. Study area

An extensive region measuring 18,000x12,000 m^2 in the northern section of the Principality of Asturias, Spain, was examined. This area is distinguished by its proximity to both an industrial and urban area, with prominent mountains and being located near the sea (see Fig. 1). Due to industrial impact, the western part of the city is significantly contaminated. Excessive levels of PM_{10} have frequently exceeded the values stipulated by legislation [26].

2.2. Geometrical model

The study's geometric model comprises a digitised terrain surface with 5-metre spatial resolution and a flat surface positioned at an altitude of 3000 metres (refer to Fig. 2). The digital surface was derived from publicly available data and preprocessed to generate an STL format file. The geometric model was scaled down to 1:10,000 to ensure dimensional equivalence with the laboratory model. A chimney measuring 70 mm (above level 0), with a total diameter of 20 mm and a concentric gas outlet measuring 10 mm in diameter, has been incorporated into the terrain of the reduced model to represent emissions in the Aboño area (as per the real model).

2.3. Numerical model

Specifically, the lower layer utilized 6 mm edge tetrahedrons up to a height of 50 mm from the ground, while the upper layer used prisms up to a level of 300 mm. The meshing of the model was accomplished using 6 mm edge tetrahedrons and prisms with a triangular base of 25 mm in height. This resulted in a total of 4,281,784 cells in the mesh. A detailed view of the mesh in contact with the ground can be observed in Fig. 3.

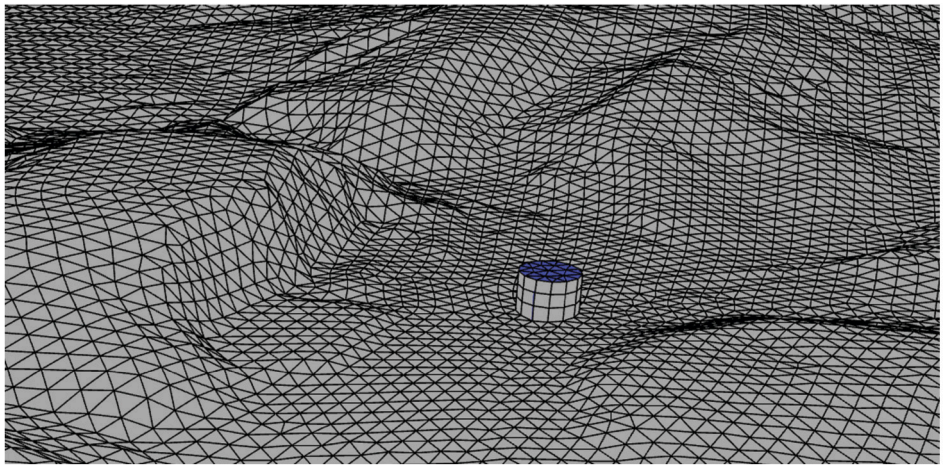

Fig. 3. Detail of the mesh in the chimney area.

The mesh quality results were deemed satisfactory, with a skew of less than 0.4. The impact of meshing was investigated, with results remaining constant for up to 10 million cells.

The Eulerian model was employed to simulate air pollutants with solid particles. This type of model is often used when there are multiple phases. It solves continuity, energy, and momentum equations for each phase, taking into consideration the occupied volume.

2.4. Input data

The model was supplied with input data, which included wind speed set at 0.4 m/s (identical to that used in the experimental tests). Additionally, the model considered the characteristics of the stack outlet flow with regard to air speed 0.05 m/s, particle volume concentration 1% and average particle size 5 microns.

2.5. Simulation conditions

Ansys Fluent 21.1 software was employed for numerical calculations. The Navier Stokes Equations were solved using the Semi-Implicit Method for Pressure-Linked Equations (SIMPLE) algorithm. The PREssure STaggering Option (PRESTO!) Scheme was used for second order temporal and spatial discretization. The turbulence model utilized was k-Epsilon-RNG.

The numerical simulation was conducted in two stages: firstly, the model was heated to reach a steady-state, and secondly, the model was subjected to a transient regime. The heating process involved introducing wind speeds at one end and atmospheric pressure conditions at the opposite end until the model reached convergence. In the simulation of the transient regime, we will introduce the chimney's outflow with the previously stated characteristics. This phase requires greater computational effort as we use a multiphase Eulerian model that accounts for air and water particles.

3. Physical model

The model was validated through a series of wind tunnel tests, utilizing a 3D printed scaled model and a particle emitter specifically manufactured for testing purposes. The four primary directions were measured using a particle meter.

3.1. Wind tunnel description

Tests were carried out at Mieres Polytechnic (annex of Oviedo university) in a wind tunnel capable of simulating the atmospheric boundary layer and reaching speeds of up to 50 m/s. This tunnel has been designed to offer great versatility in the study of aerodynamic problems (Fig. 4). It has been designed as a closed circuit, with a closed test chamber and with sufficient length to develop a boundary layer in a controlled manner. The dimensions of this tunnel allow testing of structures such as bridges, solar panels, turbines, bicycles, etc. with a high quality in the test chamber (uniform distribution of velocity and pressure for the desired flow rates and very low turbulence). In addition, it has return and discharge zones that are used as secondary test chambers, larger in size and with lower wind speed.

The main dimensions of the tunnel are 31.52 m length, 10.84 m width and a height varying between 2.54 m in the standard section and 3.48 m in the backwater chamber. The 4 fans, 1250 mm in diameter and 12 blades, are installed alongside each other, have a power of 4x45 kW and provide sufficient power to reach speeds of over 45 m/s in the test chamber.

Given the extremely low and uniform velocities required in this experiment, the tests were carried out in one of the secondary chambers corresponding to section A in Fig. 4. The discharge chamber with a square section of 2.44 m in height and a width of 2.40

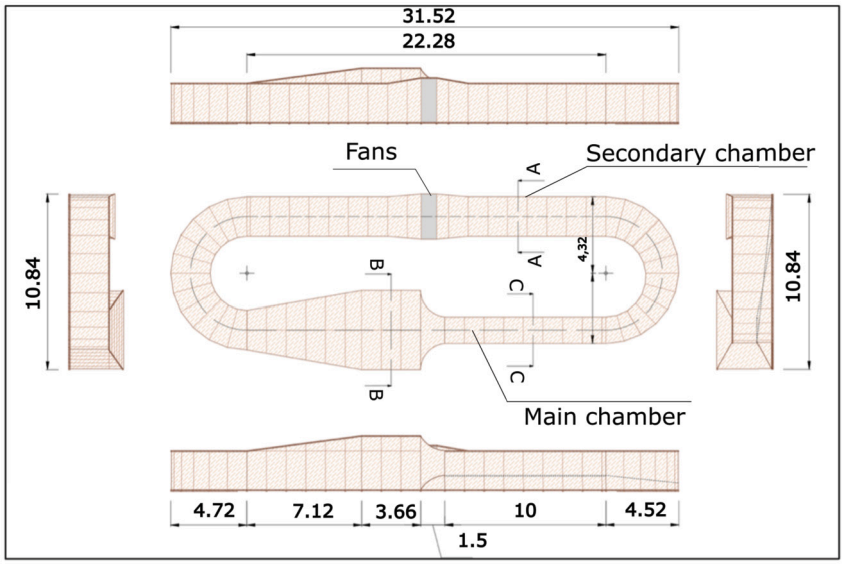

Fig. 4. General view and dimensions (in m) of the wind tunnel.

Fig. 5. View of the secondary chamber. (a) Suction of the fans. (b) Deflectors.

m was chosen (Fig. 5a). In this area the flow is less turbulent due to the effect caused by the suction of the fans and the two funnels installed (Fig. 5b).

3.2. Construction of the scale model

The first step was to define the scale and dimensions of the model. In this case, the same scale was used as in the CFD model at a reduced scale (1:10,000) and the extension was reduced to the area of greatest interest, corresponding to the western area of Gijón as it was the most affected by the particle emitting sources. The limits of the model are shown together with those of the CFD model in Fig. 6. The scale of the model was limited by wind tunnel dimensions and space needed for measurement instruments and minimum velocity in that infrastructure is 0.4 m/s. We have tried to maintain the similarity criteria as far as possible, to obtain an adequate validation of the CFD model with the physical one.

The next step was to obtain the cartography of the area for the physical model, which was generated from the Digital Terrain Model (DTM) used to build the CFD model. From the surface, a volume is constructed that allowed its physical reproduction by 3D printing, adapting to the maximum dimensions allowed by the printer (Fig. 7a). In order to get hold of a modular and scalable format, a solution based on 300x300 mm^2 squares was chosen (Fig. 7b), so 4 files in STL format will be taken to the 3D printer software. The model was performanced using additive manufacturing equipment capable of producing elements up to 400x400x400 mm^3. The chimney utilized as an emission source was positioned 70 mm above the 0 level of the model. It had a diameter of 20 mm, which produced a flow of particles that could be readily measured by the instrumentation. The chimney also featured an outlet of 10 mm.

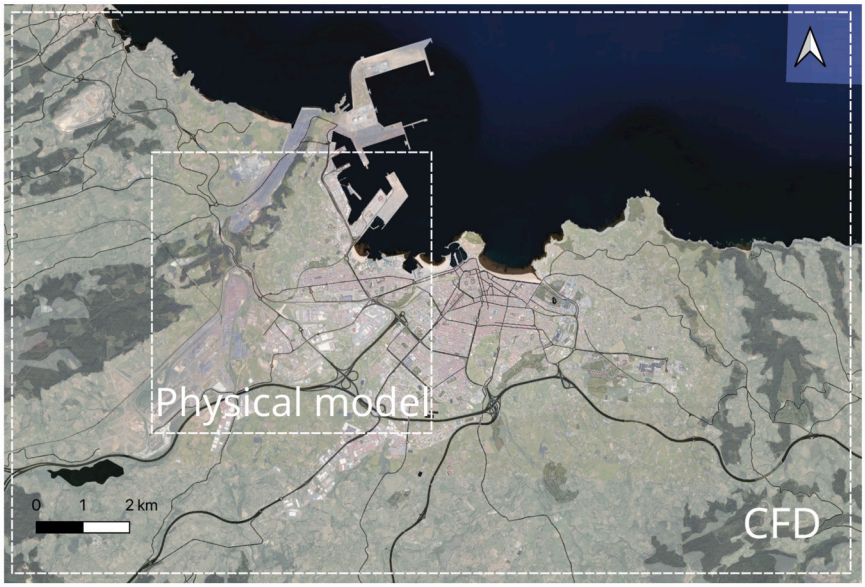

Fig. 6. Limits of the physical model and the CFD model.

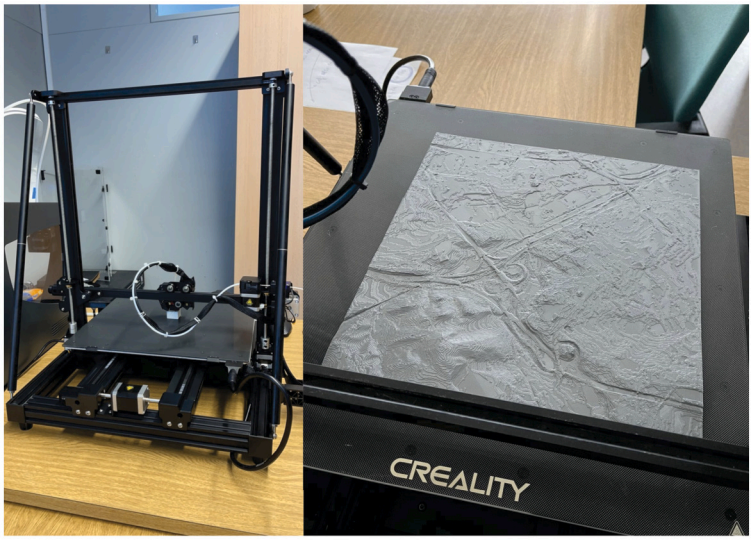

Fig. 7. (a) 3D printer. (b) Detail of one of the printed fragments.

3.3. Manufacture of a particle emitter

A particle emitter was built with a view to obtaining a small flow rate device that could be controlled in the reduced dimensions of the model and that enables to observe the effect on the orography (Fig. 8).

The following components are used for this purpose:

- Methacrylate watertight container. Two holes must be drilled in the container. The first one, below the water level, will allow the introduction of air into the closed volume. The second, at mid-height, will allow the connection of the tube that will channel the steam from the particle emitter to the model's chimney.
- Two ultrasonic nebulizers. A nebulizer is a device that atomizes a liquid into fine particles, in this case liquid water. They will be introduced inside the vessel and will be located below the water level (Fig. 9a).
- Air compressor. A SUNSUN CT series device with a power of 3 W is used to introduce a constant flow of 120 litres/hour through a 5 mm diameter tube connected to it. In this way, the output flow rate of the particle emitter will be the same as the one entering the compressor (Fig. 9b).

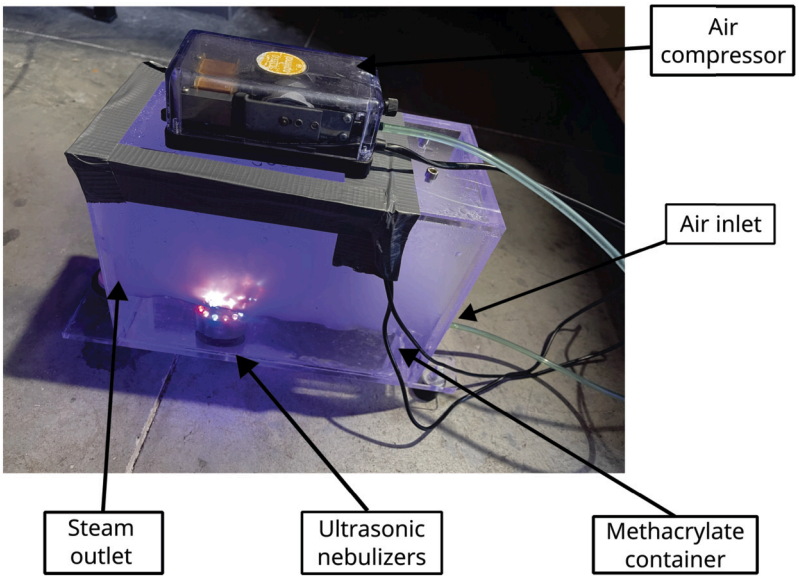

Fig. 8. Particle emitter with its components in operation.

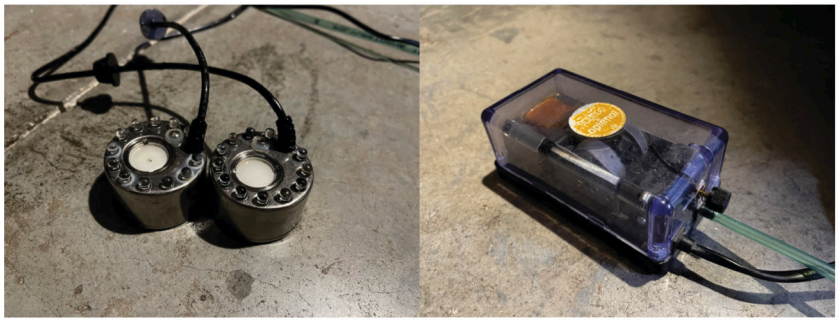

Fig. 9. (a) Ultrasonic nebulizers. (b) Air compressor.

3.4. Measuring instrumentation

During the experiment, measurements must be taken to determine the particle concentration in the model (Fig. 10). For this purpose, a TSI model 3330 portable particle meter was used (Fig. 11a). The equipment allows to measure particle concentration and size distribution every second (sampling frequency of 1 Hz). It is an optical particle sizer (OPS) that deploys state-of-the-art optics with 120º light collection, thereby improving resolution and guaranteeing high precision of the measurements. By means of individual particle counting, it is capable of detecting particles from 0.3 to 10 microns in 16 channels of user-adjustable size.

The particle meter was used in conjunction with a measuring tube. This was a holed metal tube designed to more accurately measure the particulate matter in the flow. The air flow enters at one end and at the other end there were two outlets to which the particle meter and a vacuum pump were connected (Fig. 11b). In this case, a Leybold Heraeus model Small Compact S 1.5 mini pump was used.

The measuring tube was placed on an auxiliary support made of wood that allows for the fitting of a mobile aluminium rail. In this way, the meter can be moved along the horizontal and vertical axis. The measuring tube was connected at one end to the vacuum pump and at the other to the air compressor.

3.5. Test methodology

Once the model, the emitter and the measurement instrumentation were in place, a measurement procedure was established for data collection in each direction. The objective was to know how wind and terrain influence the dispersion of the pollutant, so that the CFD methodology proposed above can be validated. The measurements consisted of creating a virtual mesh of measurements spaced every 1 cm to obtain the particle concentration values. For this purpose, samples were taken every centimetre across the width of the model (horizontal axis) and at the top (vertical axis) generating this measurement plane (Fig. 12).

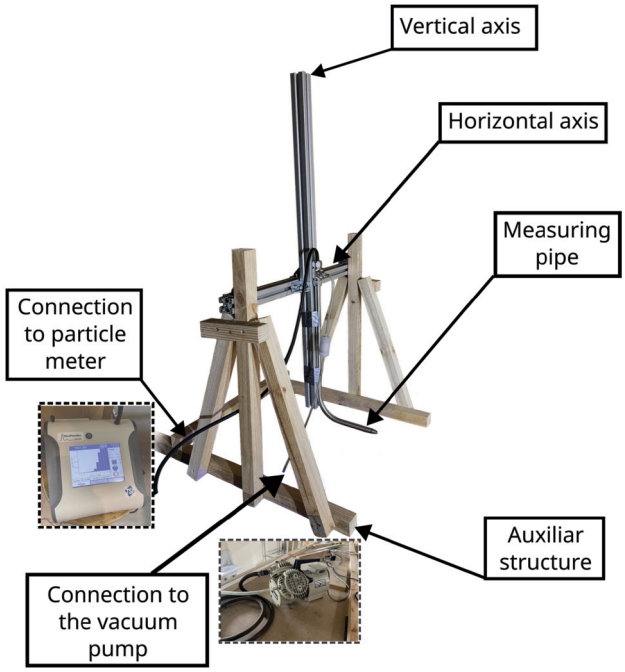

Fig. 10. Assembly of the assembly consisting of the particle meter, the measuring tube, the vacuum pump and its connections.

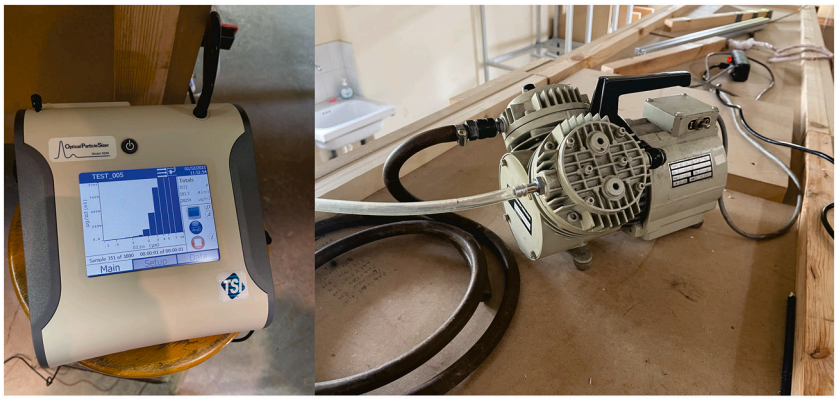

Fig. 11. (a) TSI 3330 OPS measuring equipment. (b) Vacuum pump.

1. The instrumentation and the model were placed in the position corresponding to the wind direction to be measured, assuring that characteristic of the flow particles is maintained constant in each test.
2. The measuring tube was placed at the 0 coordinate on the surface of the model and at the origin point of the horizontal axis. In order to maintain consistency in the measurements, an origin of coordinates had been previously placed and the axis had been graduated with marks every 1 cm.
3. With the tunnel turned on and the particle emitting equipment working, started the particle meter and waited for it to register the number and size distribution of the particles.
4. After the measurement corresponding to the position 0 vertical, 0 horizontal, the measuring tube was moved 1 cm horizontally, maintaining the height and the measurement was repeated. Iterated until the horizontal dimension of the model was completed.
5. At the completion of the 0 cm height, the results were saved, and steps 2 to 4 were repeated but at 1 cm from the vertical, subsequently records were taken for 2, 3 and 4 cm.
6. Once the wind direction was completed, the model was rotated to vary the incident wind direction.

Before conducting the tests, the particle emitter was simulated. The same methodology was used to measure the output concentration of the emitting source as was used to measure the particles at the base of the model. The emitting source was placed 100 mm from the measuring tube and measurements were taken in the transverse plane with the aid of the particle meter until all the

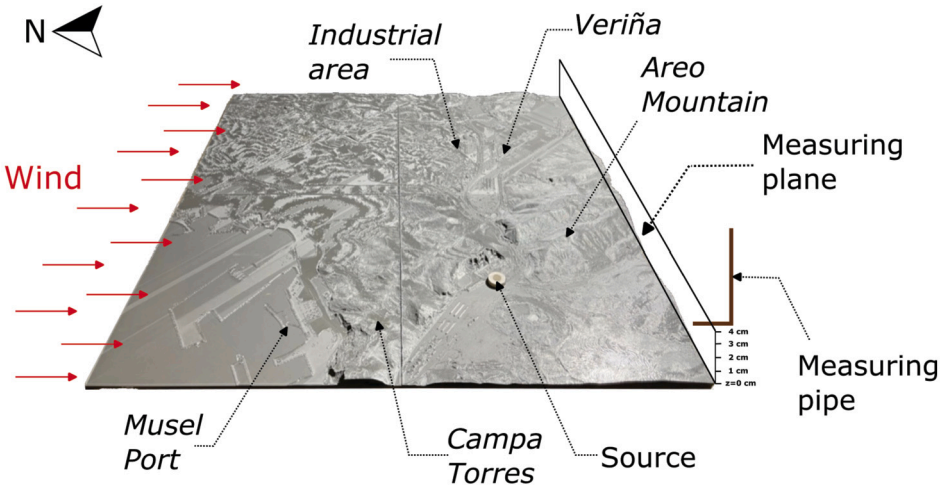

Fig. 12. Schematic structure of the layout during the tests.

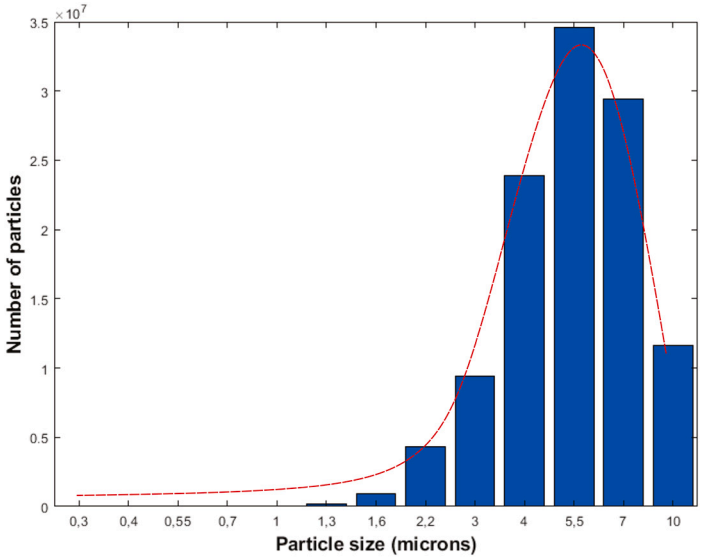

Fig. 13. Particle size distribution of the emitting source.

particles passing through it were known. Outlet flow rate (120 L/h) as it corresponded to the air pump, the outlet velocity (0.05 m/s), the section of the emitting source (10 mm inside diameter) and the section of the measuring plane chosen in this test, which will be 110x110 mm^2, were also known. Employing these data, it was possible to know the concentration of the meter, obtaining 0.01 m^3 of water/m^3 air (which can be included as a concentration in volume in the CFD simulations). Similarly, the particle distribution was analysed, obtaining an average size of 5 microns (Fig. 13).

Following this methodology, four tests were carried out corresponding to the north, south, east and west directions. Fig. 14 shows the layout of the equipment in the test chamber, the metal structure on which the measuring tube was placed and the wooden structure on which the wood was placed. The set was located in a part of the test chamber where the wind is uniform, away from the access door and the tunnel walls.

4. Results and discussion

Main wind directions (north, south, east and west) were tested because they are considered the most appropriate for this configuration of the model and the measurement instrumentation. Fig. 15 shows a profile of the model with the particle emitter on and the wind tunnel off.

The wind speed used was uniform of 0.4 m/s, which was regulated by a frequency converter and checked with a portable anemometer. The exit velocity of the particles emitter was 0.05 m/s. Those velocities were chosen so that the behaviour of the particles on the scale model would have a similar appearance to reality taking into account the orography. In this way, the particles

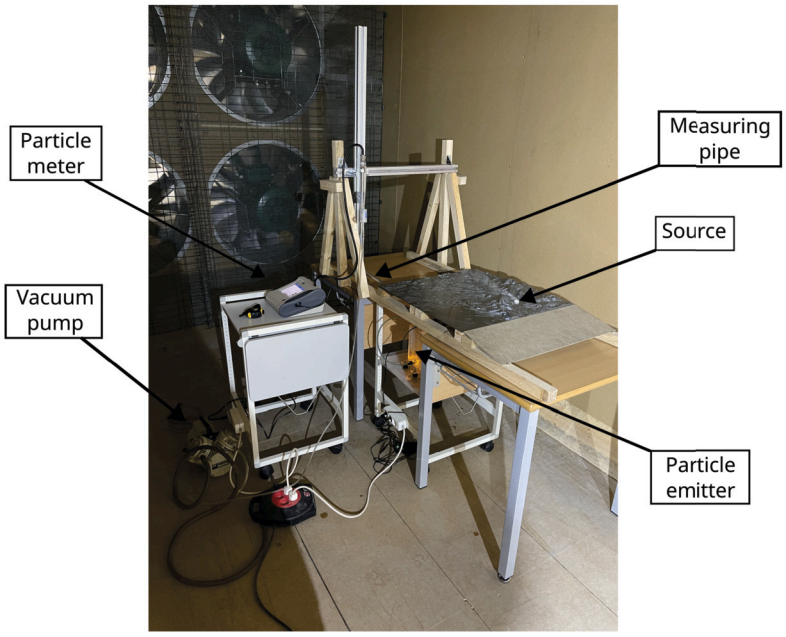

Fig. 14. Assembly carried out in the wind tunnel.

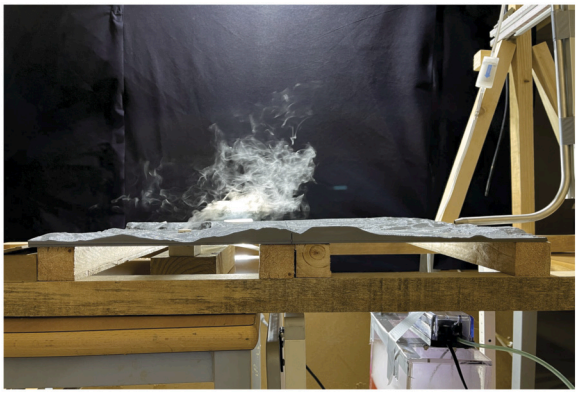

Fig. 15. Profile of the model with the particle emitter on.

released on the scale model behave in their spatial distribution in a similar way as they would in reality, with different characteristic times.

Fig. 16(a) shows how the particle flow emanating from the emitter goes through the mountains. Fig. 16(b) shows the path that the wind finds when it reaches the test model. In the background is the measuring equipment where the particle and size distribution will be obtained to calculate the concentrations.

Four CFD simulations were conducted at a reduced scale in four cardinal directions (north, south, east, and west) that corresponded to the wind tunnel testing directions. In the transient phase, each simulation utilized 500 time intervals of one second and sufficient iterations to attain residuals of lower than 10^{-5} for each governing equation. Each simulation required 100 hours of computational time on a computer equipped with a 16-core EPYC 7351P processor running Ansys Fluent 21.1 at a clock speed of 2.4 GHz. The identical input data utilized in the wind tunnel testing was employed.

The test corresponding to the north will be greatly influenced by the high regions of Campa Torres and Monte Areo, which will act as a natural barrier. A low level of particles is expected in the area of the city as it is far away from the emitting source and protected by the Campa Torres. However, the area in the immediate vicinity of the industrial estates should have higher values (Fig. 17(a)).

In the test taken from the south, the wind flows through a channel formed by Monte Areo and Campa Torres. Measurements made in that area will consequently reveal high values while in the rest of the measurement plane values closer to zero will be obtained. This particular wind direction means that the particles disperse towards the sea and do not go towards the city (Fig. 17(b)).

In the east wind test, similar results will be obtained in the measuring plane due to its geometrical arrangement (Fig. 17(c)). With the east wind, the Campa Torres acts as a natural barrier, blocking the passage of the wind and generating turbulence on both sides. The particularity of this case is that the mountain range offers three valleys (areas marked in blue) that have a real elevation between

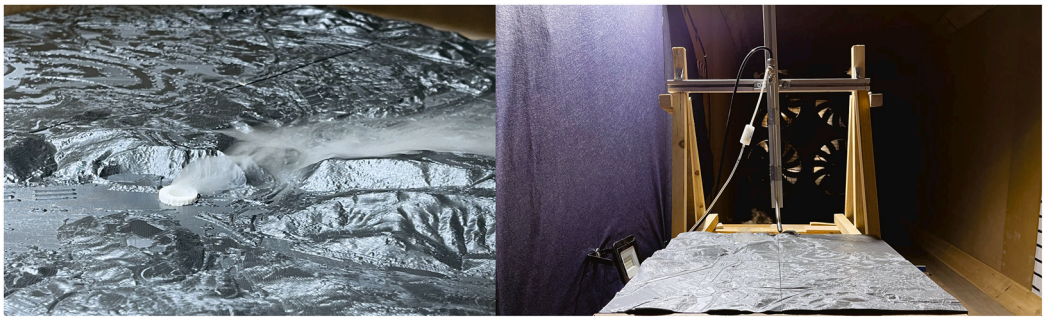

Fig. 16. (a) Detail of the particles leaving the emitting source over the orography. (b) Front view of the model with the particle emitter on with north wind.

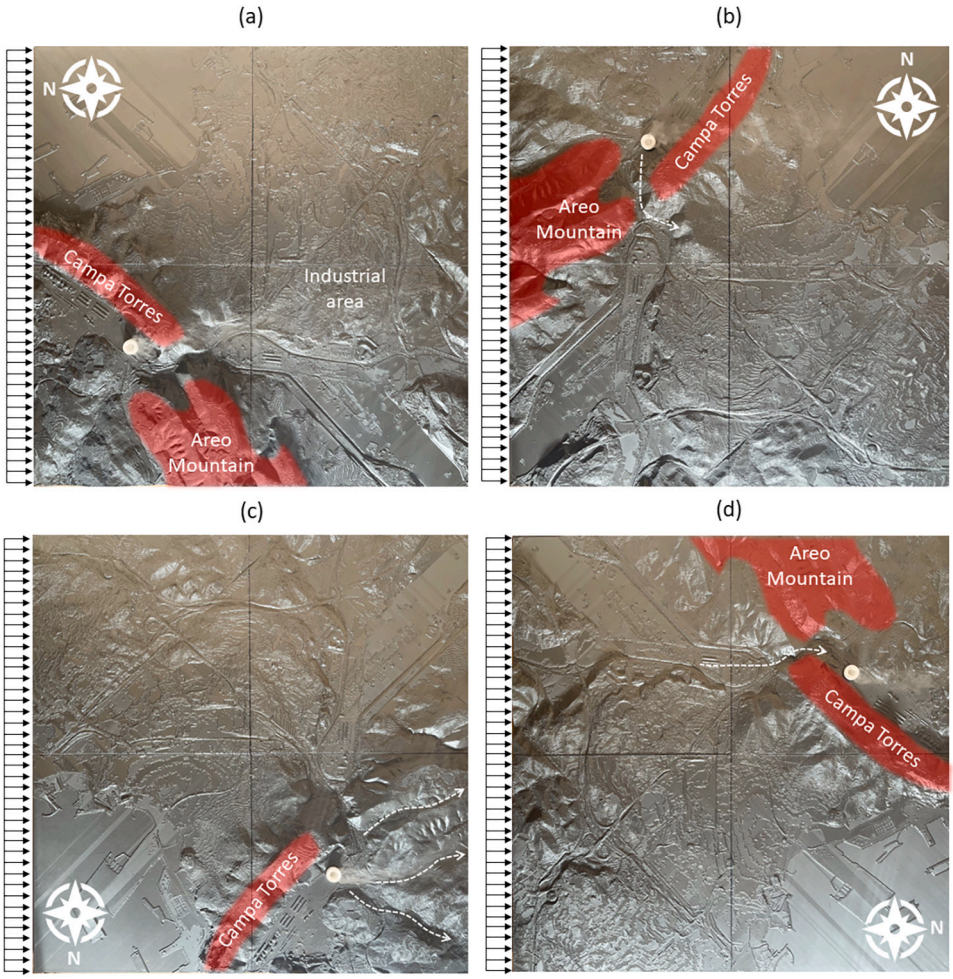

Fig. 17. Images of the top view with wind from (a) north, (b) south, (c) east and (d) west.

60 and 145 m and offer three different outlets for the pollution coming out of the emission source. In this case, the influence of the terrain, which marks the path of particle dispersion, acting as a barrier or generating natural outflow paths through the valleys, can be clearly seen.

Finally, in the west wind layout, the influence of the Campa Torres can be clearly seen as an obstacle that prevents pollutants from reaching the city. In the measurement plane, the highest values will be found further north, in the area corresponding to the Port of Musel and the Cantabrian Sea. However, due to the outflow channel formed in Veriña, part of the outflow may also reach the western part of the city. This case is the most unfavorable arrangement as it drags the pollutants from the outfall, breaching Campa Torres, and heads directly towards the city. However, it does not justify further study on a greater scale (Fig. 17(d)).

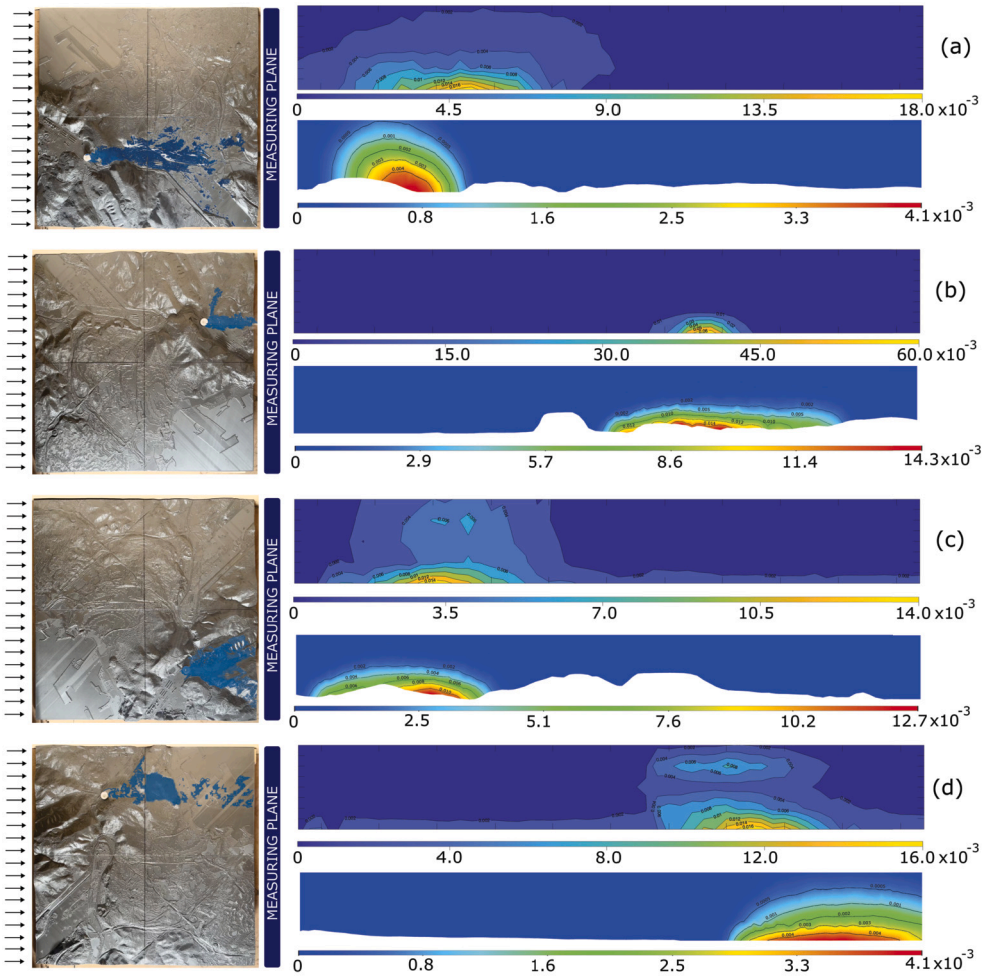

Fig. 18. Results for (a) north, (b) south, (c) east and (d) west winds. In each of them shows the experimental imagen with wind entering from the left and the comparison between dimensionless relative concentration values experimental (top right) and CFD (bottom right).

Final validation was achieved using the data obtained in the final surface of the model (area opposite to the wind inlet). For each wind direction there are three results: the experimental data obtained in the test, the CFD simulation data of the reduced model and the plan image of the test.

Four tests have been carried out in which 275 measurements of 60 s each have been taken and where the number of particles passing through each cm^2 has been carefully measured. The plane has a length of 55 cm (an edge of 3 cm was left unmeasured on both sides), with a maximum height of 4 cm above the 0 level of the model. The results show the relative value of particle concentration at each point (in percent per one).

To show the results, the raw concentration measurements have been adimensionalised by dividing them by the source output concentration. The CFD simulation values are obtained in the same way, as a dimensionless concentration value.

Fig. 18(a) shows the results with incident wind from the north. What can be clearly observed is that the dispersion is largely influenced by the channel formed between Campa Torres and Veriña. This means that most of the particles reaching the measurement plane are concentrated around the 15 cm position and at a very low level. In the simulation, a similar dispersion is obtained, with values very close to 0 between 30 and 60 cm, due to the emissions being at a fair distance and protected by the mountain. The simulation underestimates the values though they remain at the same order of magnitude (10^{-3}). According to the image, it seems, at least on the face of it, that the highest concentrations are in the industrial area, near the industrial estate of Somonte, mostly flat, where the concentration of particles from this source would increase.

In Gijón, the south wind (Fig. 18(b)) favours the dispersion of pollutants, as it carries them towards the sea. In this case it is noticeable how the wind crosses the valley and quickly leaves the domain. Experimental results show very concentrated values around the horizontal position at 40 cm. The simulation data retains the same core but considers more dispersed values at lower elevations. On the other side of the Campa Torres, the contamination has no effect on the city. Again, the CFD tends to underestimate the maximum values, with values up to four times higher. However, they maintain orders of magnitude of 10^{-3}, which is satisfactory in tests lasting longer where it is difficult to keep all variables constant.

The east wind (Fig. 18(c)) is also a favourable wind for Gijón as it avoids the arrival of particles to the city, as was already the case with the south wind. The measurements are again high, but the particles will quickly leave the domain following various trajectories created by the mountain. The peak is around 15 cm with almost equal values between the experimental and numerical values. These values occur at low altitudes, although it seems that in the experimental case the values decreased less steeply in height than in the numerical one.

Finally, in the western scenario (Fig. 18(d)), the most decisive insofar as Gijón is concerned, maximums of around 40 cm have been obtained in the experimental test and 50 cm in the simulation, where the maximum appears slightly offset. The remainder of the model continues with practically non-existent measurements, but in the case of overcoming the Campa Torres particles go directly towards the centre of the city. The maximum values are again underestimated in the CFD simulation, but the order of magnitude remains correct. The image shows how after getting beyond the mountain there is an accumulation of particles that are subsequently dispersed.

The CFD simulations at a reduced scale produce results similar to those found in the laboratory. The model can predict particle behaviour during dispersion in various wind conditions, with the simulated terrain also influencing the model. While the CFD tends to underestimate the maximum compared to experimental data, all values remained within the same order of magnitude. Additionally, the sample correlation coefficient values exceed 0.8 in all cases.

5. Conclusions

To conduct studies on the dispersion of particulate pollutants in vast areas through numerical modelling, ensuring the accuracy of the models is paramount. This study validates a numerical model of western Gijón, Spain, for its accuracy through a physical model in a wind tunnel employing a water particle emitter. The models have a scale of 1:10,000. The model has undergone testing in an aerodynamic tunnel and has been exposed to wind from four main directions. The results are satisfactory, and the numerical model demonstrates a high capability to forecast the particles' dispersion in the air. The values obtained from both the physical and CFD models are in the same magnitude.

Although the presented model has limitations (density and concentrations of particles, etc.) to extrapolate its use to real scenarios, its design is a good starting point that must be completed in future investigations to obtain a final model that can be used to evaluate the particle distribution in urban environments as well as the selection analysis of the effect of corrective measures.

CRediT authorship contribution statement

V.M. Fernández-Pacheco: Data curation, Investigation, Software, Validation, Writing – original draft, Writing – review & editing. **A. Fernández-Tena:** Formal analysis, Visualization. **T. Ackermann:** Formal analysis, Visualization. **E. Blanco-Marigorta:** Conceptualization, Project administration, Supervision. **E. Álvarez-Álvarez:** Funding acquisition, Project administration, Supervision, Writing – review & editing.

Declaration of competing interest

The authors declare that they have no known competing financial interests or personal relationships that could have appeared to influence the work reported in this paper.

Data availability statement

The measurement data published in this paper are part of the research project Severo Ochoa BP19-160 and cannot be published openly, only the publication of the results is allowed.

Acknowledgements

This work has been supported by "Severo Ochoa for research and teaching" BP19-160 scholarship provided by Principality of Asturias.

References

[1] European Environment Agency, Air quality in Europe, vol. 1, 2019.
[2] Council of the European Union, Communication from the Commission to the European Parliament, the Council, the European Economic and Social Committee and the Committee of the Regions: on the 2017 list of Critical Raw Materials for the EU, Off. J. Eur. Union COM(2017) (2017) 8.
[3] S. Larssen, L.O. Hagen, Review on requirements for models and model application, Most (November) (1996).
[4] United States Environmental Protection Agency (USEPA), Air Quality Dispersion Modeling - Preferred and Recommended Models, https://www.epa.gov/scram/air-quality-dispersion-modeling-preferred-and-recommended-models, 2021.
[5] Exponent, Official CALPUFF modeling system, http://www.src.com/, 2021.
[6] CALIOPE, Sistema CALIOPE. Sistema de pronóstico de calidad del aire, http://www.bsc.es/caliope/es, 2021.
[7] J.M. Baldasano Recio, O. Jorba Casellas, S. Gassó Domingo, M.T. Pay Pérez, G. Arevalo Roa, CALIOPE: sistema de pronóstico operacional de calidad del aire para Europa y España, in: XXXII Jornadas Científicas de la Asociación Meteorológica Española. Meteorología y Calidad del Aire, 2012, pp. 1–6, www.bsc.es/caliope.

[8] S. Brusca, F. Famoso, R. Lanzafame, S. Mauro, M. Messina, S. Strano, PM10 dispersion modeling by means of CFD 3D and Eulerian–Lagrangian models: analysis and comparison with experiments, Energy Proc. 101 (2016) 329–336, https://doi.org/10.1016/J.EGYPRO.2016.11.042, https://www.sciencedirect.com/science/article/pii/S1876610216312516.

[9] S.M. Salim, R. Buccolieri, A. Chan, S. Di Sabatino, Numerical simulation of atmospheric pollutant dispersion in an urban street canyon: comparison between RANS and LES, J. Wind Eng. Ind. Aerodyn. 99 (2–3) (2011) 103–113, https://doi.org/10.1016/J.JWEIA.2010.12.002, https://www.sciencedirect.com/science/article/pii/S0167610510001248.

[10] X. Zheng, J. Yang, CFD simulations of wind flow and pollutant dispersion in a street canyon with traffic flow: comparison between RANS and LES, Sustain. Cities Soc. 75 (August) (2021) 103307, https://doi.org/10.1016/j.scs.2021.103307.

[11] K. Ahmad, M. Khare, K.K. Chaudhry, Wind tunnel simulation studies on dispersion at urban street canyons and intersections - a review, J. Wind Eng. Ind. Aerodyn. 93 (9) (2005) 697–717, https://doi.org/10.1016/j.jweia.2005.04.002, www.elsevier.com/locate/jweia.

[12] P.Y. Cui, Z. Li, W.Q. Tao, Numerical investigations on Re-independence for the turbulent flow and pollutant dispersion under the urban boundary layer with some experimental validations, Int. J. Heat Mass Transf. 106 (2017) 422–436, https://doi.org/10.1016/j.ijheatmasstransfer.2016.08.038.

[13] F. Xue, X. Li, The impact of roadside trees on traffic released PM10 in urban street canyon: aerodynamic and deposition effects, Sustain. Cities Soc. 30 (2017) 195–204, https://doi.org/10.1016/J.SCS.2017.02.001, https://www.sciencedirect.com/science/article/pii/S2210670716304528.

[14] Y. Zhang, Z. Gu, C.W. Yu, Impact factors on airflow and pollutant dispersion in urban street canyons and comprehensive simulations: a review, https://doi.org/10.1007/s40726-020-00166-0, 2020.

[15] A. Wania, M. Bruse, N. Blond, C. Weber, Analysing the influence of different street vegetation on traffic-induced particle dispersion using microscale simulations, J. Environ. Manag. 94 (1) (2012) 91–101, https://doi.org/10.1016/j.jenvman.2011.06.036, www.envi-met.com.

[16] R. Buccolieri, C. Gromke, S. Di Sabatino, B. Ruck, Aerodynamic effects of trees on pollutant concentration in street canyons, Sci. Total Environ. 407 (19) (2009) 5247–5256, https://doi.org/10.1016/j.scitotenv.2009.06.016, http://www.

[17] J.L. Santiago, R. Buccolieri, E. Rivas, H. Calvete-Sogo, B. Sanchez, A. Martilli, R. Alonso, D. Elustondo, J.M. Santamaria, F. Martin, CFD modelling of vegetation barrier effects on the reduction of traffic-related pollutant concentration in an avenue of Pamplona, Spain, Sustain. Cities Soc. 48 (October 2018) (2019) 101559, https://doi.org/10.1016/j.scs.2019.101559.

[18] Y.d. Huang, M.z. Li, S.q. Ren, M.j. Wang, P.y. Cui, Impacts of tree-planting pattern and trunk height on the airflow and pollutant dispersion inside a street canyon, Build. Environ. 165 (2019), https://doi.org/10.1016/j.buildenv.2019.106385.

[19] C. Gromke, A vegetation modeling concept for building and environmental aerodynamics wind tunnel tests and its application in pollutant dispersion studies, Environ. Pollut. 159 (8–9) (2011) 2094–2099, https://doi.org/10.1016/j.envpol.2010.11.012.

[20] H. Yang, C.K.C. Lam, Y. Lin, L. Chen, M. Mattsson, M. Sandberg, A. Hayati, L. Claesson, J. Hang, Numerical investigations of Re-independence and influence of wall heating on flow characteristics and ventilation in full-scale 2D street canyons, Build. Environ. 189 (2021) 107510, https://doi.org/10.1016/j.buildenv.2020.107510.

[21] V. Garbero, P. Salizzoni, L. Soulhac, Experimental study of pollutant dispersion within a network of streets, Bound.-Layer Meteorol. 136 (3) (2010) 457–487, https://doi.org/10.1007/s10546-010-9511-2.

[22] P. Michálek, D. Zacho, Wind tunnel measurement of flow and dispersion over urban area, EPJ Web Conf. 143 (2017), https://doi.org/10.1051/epjconf/201714302074.

[23] M.F. Yassin, S. Kato, R. Ooka, T. Takahashi, R. Kouno, Field and wind-tunnel study of pollutant dispersion in a built-up area under various meteorological conditions, J. Wind Eng. Ind. Aerodyn. 93 (5) (2005) 361–382, https://doi.org/10.1016/j.jweia.2005.02.005, www.elsevier.com/locate/jweia.

[24] P.Y. Cui, Z. Li, W.Q. Tao, Wind-tunnel measurements for thermal effects on the air flow and pollutant dispersion through different scale urban areas, Build. Environ. 97 (2016) 137–151, https://doi.org/10.1016/j.buildenv.2015.12.010.

[25] B. Xin, W. Dang, X. Yan, J. Yu, Y. Bai, Dispersion characteristics and hazard area prediction of mixed natural gas based on wind tunnel experiments and risk theory, Process Saf. Environ. Prot. 152 (2021) 278–290, https://doi.org/10.1016/j.psep.2021.06.012.

[26] MITECO, Evaluacion de la Calidad del Aire en Espana, 2018, p. 208, https://www.miteco.gob.es/es/calidad-y-evaluacion-ambiental/ temas/atmosfera-y-calidad-del-aireinformeevaluacioncalidadaire espana2018tcm30-498764.pdf.

[27] V.M. Fernández-Pacheco, E. Álvarez-Álvarez, E. Blanco-Marigorta, T. Ackermann, CFD model to study PM_{10} dispersion in large-scale open spaces, Sci. Rep. 13 (1) (2023) 5966, https://doi.org/10.1038/s41598-023-33144-9.